559400

AIAA-2001-4383

DYNAMICS AND STABILITY AND CONTROL CHARACTERISTICS OF THE X-37

A. Chaudhary*, V. Nguyen†, H. Tran‡, D. Poladian§, and E. Falangas*
Boeing Phantom Works

Abstract

This paper presents the stability and control analysis and the control design results for the Boeing/NASA/AFRL X-37. The X-37 is a flight demonstrator vehicle that will go into space and after its mission, autonomously reenter and land on a conventional runway. This paper studies the dynamics and control of the X-37 from atmospheric reentry through landing. A nominal trajectory that lands on the Edwards Air Force Base Lakebed is considered for all the analysis and design. The X-37's longitudinal and lateral/directional bare-airframe characteristics are presented. The level of maneuvering control power is assessed. Vehicle trim with multiple surfaces is discussed. Special challenges where the wings loose roll effectiveness are discussed and solutions are presented. Aerodynamic uncertainties and flexibility modeling issues are presented. Control design results and robustness analysis methods are presented. Results are provided for the Entry, Terminal Area Energy Management (TAEM), and Approach and Land phases.

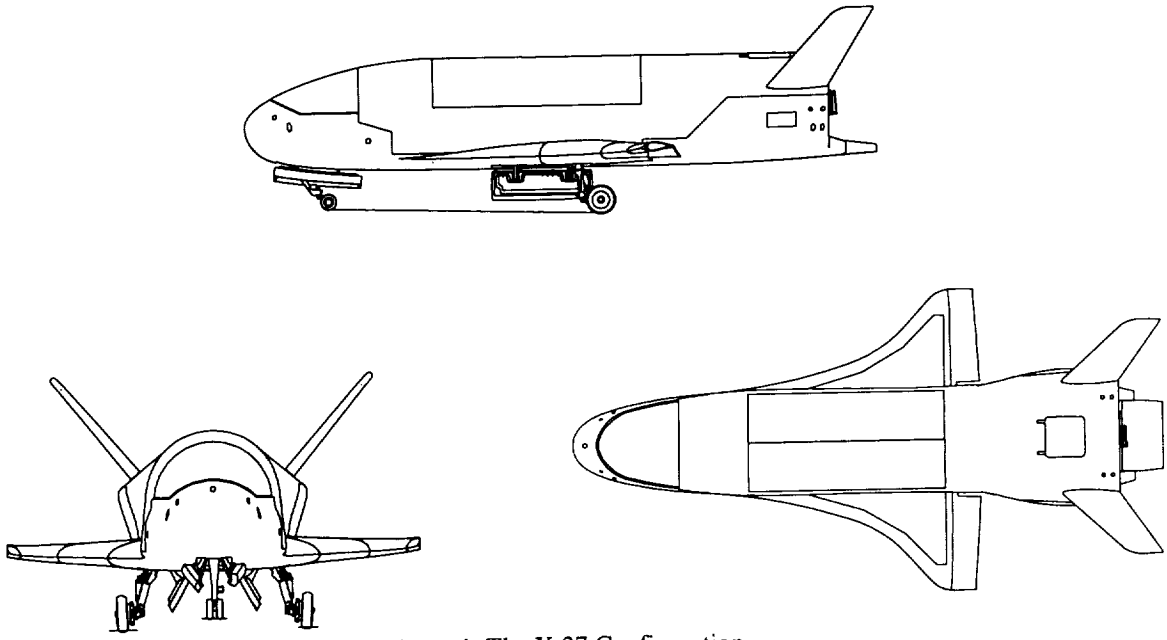

Figure 1, The X-37 Configuration

* Principal Engineer
† Boeing Tech. Fellow, and Lead GN&C
‡ Principal Engineer, AIAA Senior Member
§ Engineering Specialist

 NASA support per Cooperative Agreement NCC8-190 is acknowledged.

Introduction

The Boeing/NASA/AFRL X-37, as shown in Figure 1, is part of the Future-X Pathfinder program. The Future-X Pathfinder Program is designed to field flight vehicles and technologies quickly and inexpensively, and to use them in reliable and safe flight operations. The goal is to advance the state of the art in low cost, reusable launch vehicle technologies that are ready, through flight-testing and qualification, to be applied to operational systems.

An important predecessor to the X-37 program was the X-40A flight test program [1]. Boeing first flight-tested the X-40A in 1998, and a majority of the analysis and design methodologies presented here were tested and validated in that program. The X-37 provides Orbital test and return capability that is new to all the other current X programs.

A successful X-37 configuration is the result of numerous iterations between multiple disciplines. The stability and control analysis presented here supports the evolution of the design to help provide an optimal design.

Control Effectors

Figure 2 shows the atmospheric control surfaces available for flight stabilization and maneuvering.

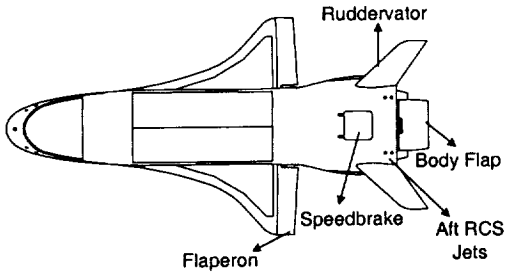

Figure 2 - Atmospheric Control Effectors

The Ruddervators provide pitch control when deflected symmetrically (de) and yaw control when deflected asymmetrically (dr). The Flaperons are for providing roll when deflected asymmetrically (da) and drag modulation when deflected symmetrically (Flaps). The Body Flap is used primarily for trimming, but it can be used as a control device to assist in pitch maneuvering. The Speedbrake is used to do drag (velocity and flight path) control in the TAEM and approach and land phases.

During reentry, aft-located jets are used to assist in trim and control. Figure 3 shows the locations of the multiple, aft jets that are used. There is roll-yaw coupling and impingement force interaction as the jets are fired. The X-37 control system is designed to manage the redundant jets and compensate for the non-linearities.

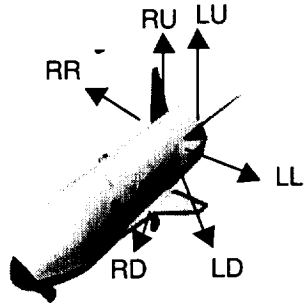

Figure 3 - Locations of the Aft RCS jets

Trajectory

The dynamic pressure and angle-of-attack of the nominal trajectory are shown as a function of Mach Number in Figure 4.

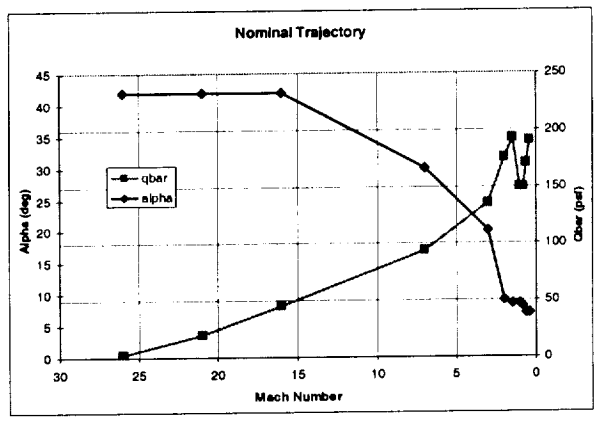

Figure 4 – X-37 Nominal Trajectory

The nominal trajectory consists of a 42-degree angle-of-attack profile after entry from an orbital inclination. The angle-of-attack flown is a trade between heat load, heat rate, range, and cross range, and it is modulated as required until the Approach and Land phase.

In the initial part of the trajectory, the bank angle is used to control drag and stay below the heat rate limit.

The X-37 has a cross range modulation capability and roll reversals are used to control cross range.

Off-nominal trajectories and variations about them are also considered in the full design cycle, but for the kind of results shown in this paper, an analysis about the nominal trajectory provides a good overall understanding.

Bare Airframe Stability and Control Characteristics

Trim Characteristics

In the upper part of the trajectory, just after reentry where the atmosphere is very thin, the X-37 uses jets, Flaps, Ruddervators, and Body Flap as needed to trim out the longitudinal dynamics. As the dynamic pressure rises, the Body Flap and Ruddervators alone are used to trim all the way to touchdown. The Body Flap and Ruddervator combination was sized such that the only small deflections of the Ruddervator are used for trimming. Figure 5 shows the deflections required, as a percentage of full authority, to trim out the longitudinal dynamics. At each analysis point in the trajectory, the vehicle was trimmed for forward and aft center-of-gravity (CG) variations combined with trajectory perturbations. The maximum deflection for the Ruddervator and Body Flap that resulted from these variations is shown in Figure 5.

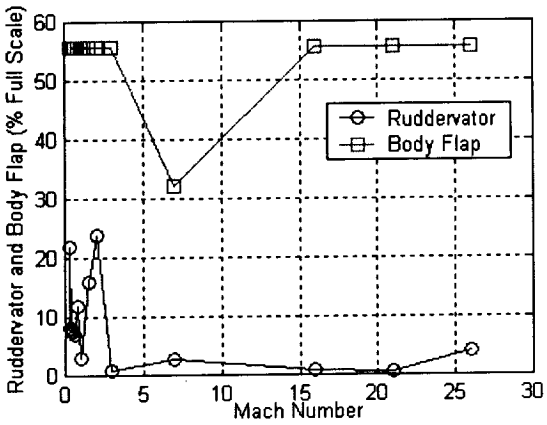

Figure 5 – X-37 Pitch Trim Authority

As shown in Figure 5, there is sufficient pitch authority during the flight envelope. The trim schedule is able to accommodate changes in the CG and other uncertainties. The Ruddervator deflection is minimal such that there is enough deflection left over for control.

Vector diagrams that plot rolling moment coefficients against the yawing moment coefficients can assess Lateral/Directional trim authority. In such diagrams, the vectors that represent the aileron, rudder, angle-of-sideslip, CG in the y direction, and jet rolling and yawing can be drawn to size up the lateral/directional trim authority. The size of the uncertainty on each vector can also be included in the diagram. Figure 6 shows such a normalized vector diagram at subsonic speeds. The boxes at the end of the vectors represent uncertainties. It can be seen that the aileron and rudder vectors can add up to cancel the dynamics created due to the angle-of-sideslip and asymmetries due to the y CG. At subsonic speeds, the jet vector is short and does not have any authority. At hypersonic speeds when the dynamic pressure is very low, the jet vector is very effective and is responsible for trimming and controlling the X-37. As illustrated in Figure 6, the aileron (da) vector swings from the right side to the left, with ramifications for controllability that are discussed later.

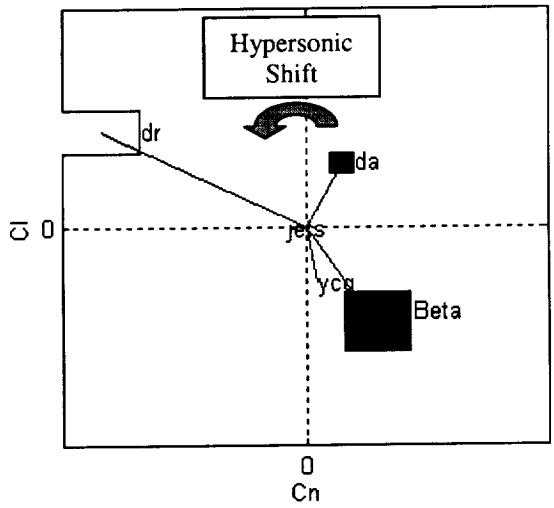

Figure 6 – Lateral/Directional Trim Authority

The Speedbrake and the Flaps are modulated for drag control, which is required for headwind and tailwind compensation. Ideally, the Ruddervator's deflection, as it holds trim, should change only slightly as the Speedbrake and Flaps are modulated. Large changes in deflection would use up all the deflection budgets as well as require gain schedules to be a function of the Speedbrake and Flaps. Figure 7 shows the change in Ruddervator required along the trajectory for full deflections of the Flaps and Speedbrake. As can be seen from Figure 7, full deflections of the Speedbrake and Flaps require only a 5 to 10% change in the Ruddervator deflection. At lower Mach numbers, where drag

modulation is most active, the change in Ruddervator deflection is even less.

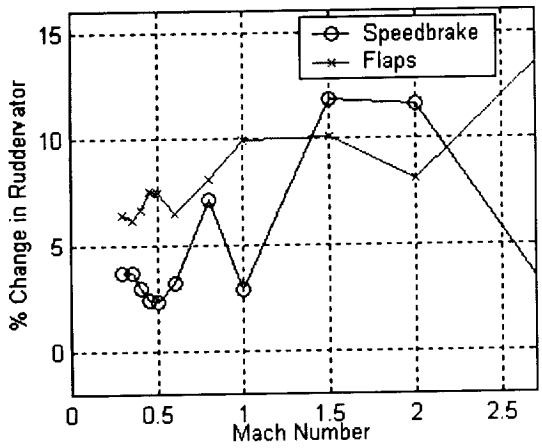

Figure 7 – Effect On Trim Of Other Surfaces

Dynamic Characteristics

The short period and phugoid modes of the X-37 along the nominal trajectory space are shown in Figure 8. The vehicle is stable along the nominal trajectory with the short period mode frequencies increasing as the dynamic pressure increases with decreasing altitude. As shown, some combinations of angle-of-attack in the transonic region give an unstable airframe, but analysis shows that there is sufficient control power for stability augmentation.

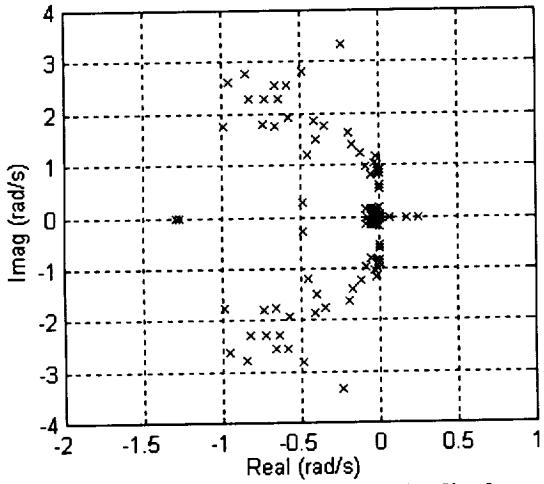

Figure 8 – Bare Airframe Longitudinal Eigenvalues

Figure 9 presents the eigenvalues of the lateral/directional bare airframe that correspond to the dutch roll, spiral, and the roll modes. The dutch roll mode can be seen as a low damped, low frequency mode. The dutch roll gets unstable at lower mach numbers, although the amount of instability can be handled by the control power available.

The maximum instability as shown in Figures 8 and 9 can be related to static margins and mode times-to-double and used to size a configuration.

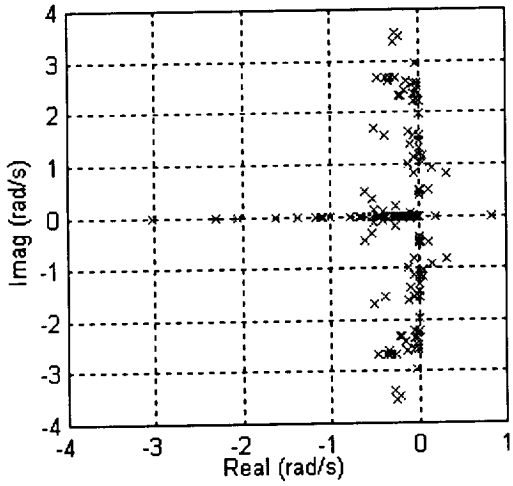

Figure 9 – Bare Airframe Lateral/Directional Eigenvalues

After trimming, there must be sufficient control acceleration left over for maneuvering. All along the trajectory, at trimmed conditions, surface deflections, required to generate a minimum acceleration to execute maneuvers demanded by guidance, were computed. The results are shown in Figure 10 along with a limit line that shows that solutions above that line will require jet assistance in order to prevent saturating the surfaces.

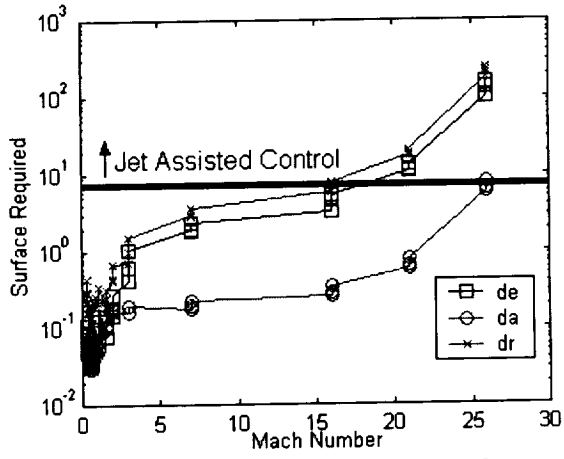

Figure 10 – Surface Deflections Required to Produce Minimum Acceleration

From the results, it can be seen that there is sufficient maneuvering authority to produce

accelerations as required. At the very high Mach Numbers, the amount of surfaces required to produce accelerations gets prohibitively high. This is due to the low dynamic pressure at these high Mach Numbers and the resulting low surface effectiveness. In the high Mach Number region, jets are used to assist in maneuvering.

Stability Derivatives

Ultimately, it is the vehicle transfer function eigenvalues and transmission zeros that determine exact open loop stability and maneuverability. However, there is a long history of looking at the vehicle's pitch, directional, and lateral stability derivatives to get a quick idea of the configuration at hand.

Looking at these derivatives assists in quickly sizing up the configuration and examining any special regimes from a stability and control perspective.

From the trim vectors presented in Figure 6, it can be seen that at subsonic speeds, the X-37 has a -Clβ (stable), a +Cnβ (stable), and that adverse roll is provided by the rudder and proverse yaw by the aileron. This section shows the characteristics of the configuration as a function of Mach Number along the trajectory.

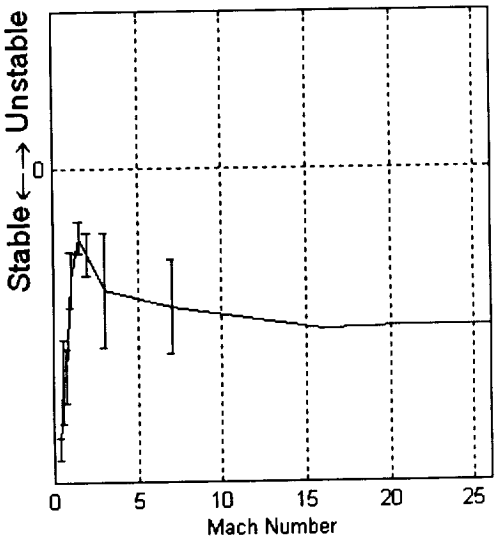

Figure 11 – Lateral Stability Derivative, Clβ

Figure 11 shows the lateral stability derivative, Clβ, as function of Mach Number for three different trajectory cases, presented as error bars about the nominal trajectory values. It can be seen that Clβ is stable throughout the trajectory.

Figure 12 shows the weather cock stability or the directional stability derivative, Cnβ, for the flight regime to be mostly negative. Again, three trajectory cases are presented as error bars about the nominal trajectory. The negative values of Cnβ do not necessarily imply instability, for Cnβ dynamic includes the effect of angle-of-attack and presents a more accurate measure of stability.

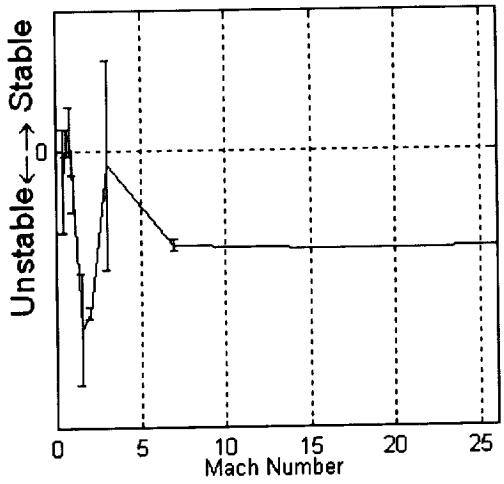

Figure 12 – Directional Derivative, Cnβ

Cnβ dynamic, as shown in Figure 13, shows that there are some regions of instability, depending on the Mach and Alpha combinations. It is for these regions that control power availability must be checked. Figure 13 also compares well with the instability level shown by the dutch roll eigenvalues for the nominal trajectory in Figure 9.

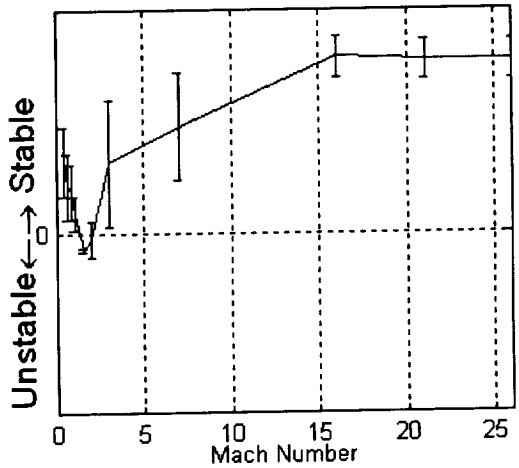

Figure 13 – Directional Derivative, Cnβ dyn, With Alpha Effects

LCDP Transition Region

As the X-37 goes from high angles of attack in the entry phase to the lower angle-of-attacks in the TAEM phase, the airflow over the Flaperons causes a change in roll responses (reversal to normal) and starts creating proverse yaw by the aileron. This is a critical region since it is not known exactly when the Flaperons will go through this change, but they must still carry out a minimal level of maneuvering.

This phenomenon can be graphically observed by looking at Figure 6, presented earlier. As the aileron vector swings from the left to the right quadrant (from hypersonic to transonic), Cnδa becomes zero and changes signs. This change in Cnδa, in combination with Clβ, causes a change in roll responses. Finally during this transition period for Cnδa, when it is exactly in line with the beta vectors, no roll rate control occurs. Fortunately, during all this, the rudder derivatives do not change sign and do not cause alignment problems with the beta vector.

Algebraically, it is seen that the Lateral Control Departure Parameter may be defined as[2]:

$$LCDP = (Cn_\beta - \frac{Cl_\beta Cn_{\delta a}}{Cl_{\delta a}}) \quad [1]$$

During the transition from high to low angle-of-attacks, the LCDP changes signs. As it changes signs, there is a period where there is no roll effectiveness from the aileron. To see why this is so, consider the transfer function relating the aileron to the roll rate:

$$\frac{p}{\delta a} = \frac{\frac{\bar{q}SbCl_{\delta a}}{Ixx}[s^2 + \frac{\bar{q}Sb}{Izz}(Cn_\beta Cos(\alpha) - \frac{Cl_\beta Cn_{\delta a}}{Cl_{\delta a}} Cos(\alpha))]}{s(s^2 + \bar{q}Sb(\frac{Cn_\beta Cos(\alpha)}{Izz} - \frac{Cl_\beta Sin(\alpha)}{Ixx}))} \quad [2]$$

The LCDP term appears in the numerator of the transfer function, and as the LCDP changes signs, the zero in the transfer function goes from the left-hand plane to the right hand plane. However due to aerodynamic uncertainties, there is a wide region in the trajectory where the numerator zero is near zero in the right hand plane and the aileron can't be counted on for any performance.

Figure 14 shows the change in the LCDP parameter for the aileron and for the Ruddervator. In closed loop control, the two may also be combined with an aileron to rudder interconnect gain, if required.

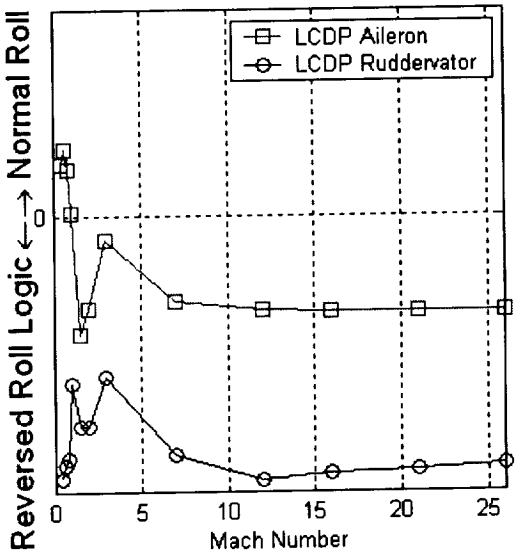

Figure 14 – LCDP of the aileron changes signs

Finally, Figure 15 shows that the derivative, $cn_{\delta a}$, changes signs and may be unknown, due to uncertainties, for a large region around the LCDP transition region. $Cn_{\delta r}$ is always produces adverse yaw and can be counted on in any control startegy.

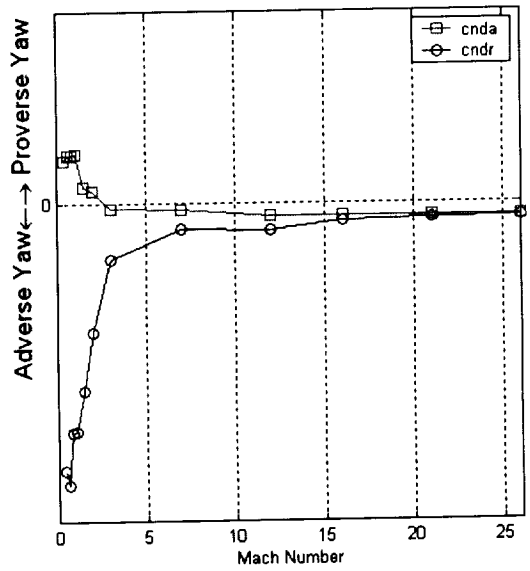

Figure 15 – cnδa reversals and predictable $cn_{\delta r}$

The control solution for this region is to not use the Cnδa derivative based gains and to use the powerful control available from the

Ruddervators when the aileron goes through the roll response change. The uncertainties in this area will have to be scrutinized and good robustness shall have to be provided by the control system.

Flexible Characteristics

It is extremely important to characterize the flexible vehicle properties since effects of the surface panels, the linkages, the actuators, and the backup structure must be understood.

The system must be specified and designed such that the first surface mode is above the actuator bandwidth frequency. Any mode frequency must be the combined contribution of the end-to-end system.

A detailed aero-elastic analysis is being done with Generalized Aerodynamics Force Derivatives (GAFD) data, which is used to model the dynamic effects of aero-elasticity. GAFD data provides coefficients that describe how the vehicle basic aerodynamic forces and moments are affected by modal displacements and rates. A second set of coefficients describes how the modal displacement of a flex mode is excited by the vehicle motion. A third set of coefficients describes how the moments at the hinges of the control surfaces are affected by changes in attitudes, rates, and deflections.

Ruddervator analysis has shown that there is a torsional and a "diving board "mode. The "diving board" mode frequency is above control frequencies and is not affected by the actuator and back-up stiffnesses.

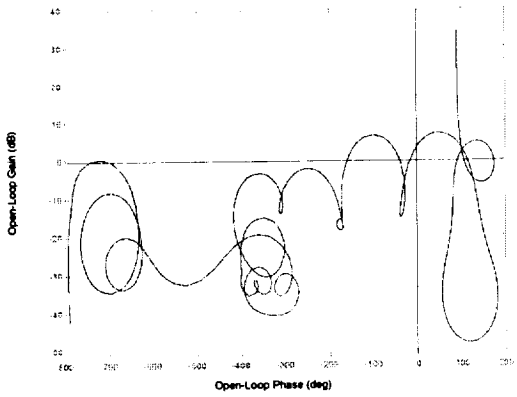

Figure 16 – Flex Model, Longitudinal Axis

The results for the other modes shown in the Nichols plots of Figures 16 and 17 indicate that there is a significant amount of bending between the rudders and the sensors in both pitch and lateral axes, and that active gain compensation must be used to attenuate the modes.

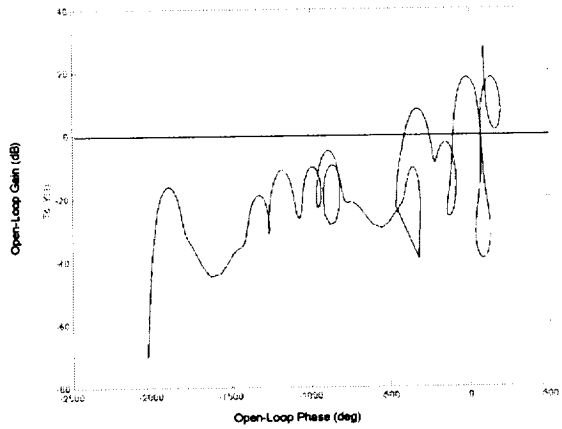

Figure 17 – Flex Model, Lateral/Directional Axis

Controls

The design was performed using Hinfinity controls and a fixed gain structure. The Hinfinity setup allows the attachment of uncertainties into the synthesis model and allows for a faster turnaround time.

Aerosurface Control

The X-37 lateral/directional control system is a roll rate demand system. Cross range is controlled by the guidance by demanding bank angle tracking, which in turn demands a crisp roll rate response.

The X-37 rolls about the stability axis to minimize the angle-of-sideslip while maneuvering. Ideally, the angle-of-sideslip should be kept as small as possible because of increased non-linearities in the vehicle dynamics with increasing angle-of-sideslip. Since the angle-of-sideslip is not available on an atmospheric reentry vehicle due to the high temperatures that would burn off any probe, the angle-of-sideslip is estimated from the side acceleration. The control system is designed to decouple, to the maximum extent possible while meeting other requirements, the roll rate responses and the angle-of-sideslip. Inertial turn compensation along with the estimated angle-of-sideslip feedback is used to obtain a coordinated roll.

Figure 18 shows the roll rate step responses for the Approach and Land, Terminal Area Energy Management, and Entry flight phases. These

responses have been superimposed on a requirements envelope developed for the Space Shuttle. Step responses are a good way to gauge whether the control system will meet the tracking and speed demands of the guidance outer loops and whether the response times will be fast enough for maneuvers executed without the guidance in the loop.

The responses for the X-37 in all phases are crisper than those demanded by the shuttle. The final responses for the X-37 will be a trade off between what the guidance demands and what can be given due to requirements of robustness and other design constraints.

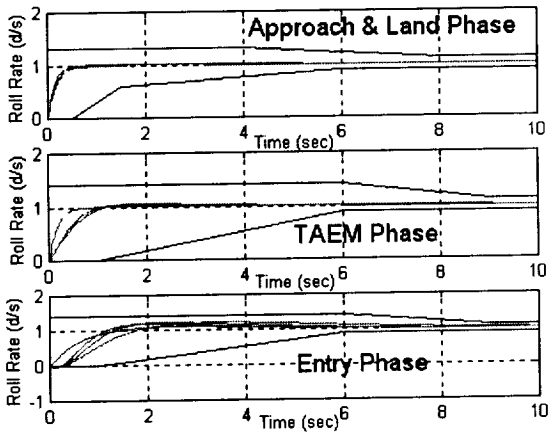

Figure 18 – Roll Rate Response in the 3 Phases

In the longitudinal axis, the flight controls uses pitch rate and normal acceleration feedback for low supersonic and subsonic flight. In the hypersonic and high supersonic regimes, pitch rate and estimated angle-of-attack feedback is used. The angle-of-attack is estimated from inertial velocities and is used for feedback, gain scheduling, and conversion of body rates to stability axis rates. However, the accuracy required on the angle-of-attack is not critical because of the high inertial velocities in the hypersonic regime and the slow variation of the aerodynamics with angle-of-attack when it is used for gain scheduling.

Figure 19 shows the normal acceleration and angle-of-attack responses from the three phases. In the Approach and Land and TAEM phases, normal acceleration responses to steps commanded by guidance are shown. Higher up, in the Entry part of the trajectory, responses to step commands in the angle-of-attack are shown.

The time domain responses in the longitudinal axis show that there is enough control power to meet requirements. Step responses such as these also help form a controls budget to show that adequate surfaces are available for both trim and control. The control system has been flown on the 6 Degree-Of-Freedom (6DOF) simulation and has helped many trajectory, actuation, and other subsystem sizing studies.

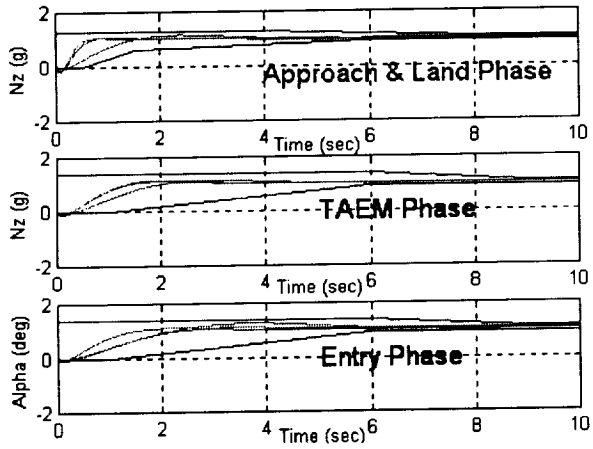

Figure 19 – Nz and Alpha Responses in the 3 Phases

Blended Aerosurface and Jet Control

Figure 20 plots the dynamics and controls vectors from the hypersonic region. It shows that the jets are a very powerful device for lateral/directional control in the region when the aerosurfaces are becoming effective for control. As scaled on the plot, only half of the jet vector is shown, and it is enough to control dynamics due to the angle-of-sideslip.

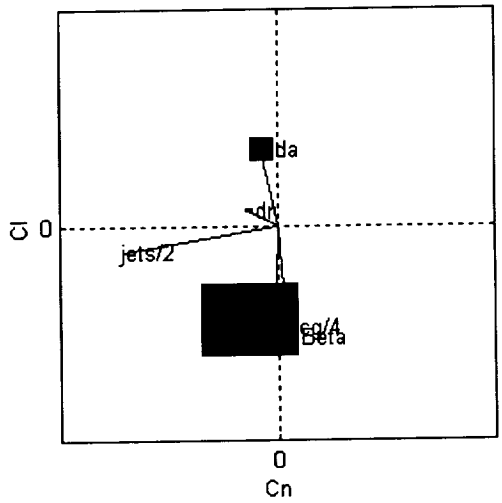

Figure 20 – Jet Control Authority

The jets were represented using results from describing function analysis and gains were designed with the same methodology as that for the aerosurfaces.

Figures 21 and 22 show the attitudes and rates during a bank angle maneuver, and the amount of jet firings required to complete the maneuver.

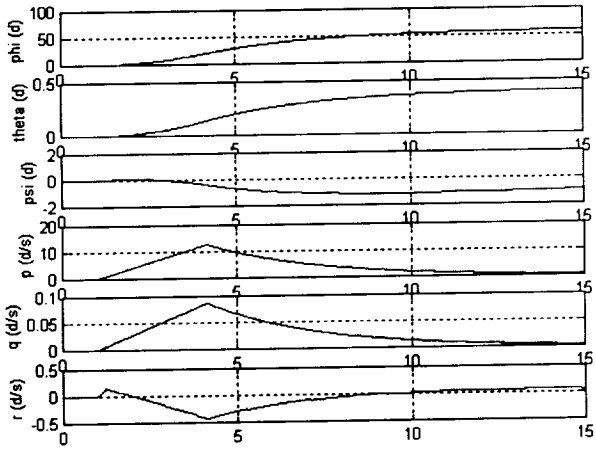

Figure 21 – Rate Contol during the upper Trajectory

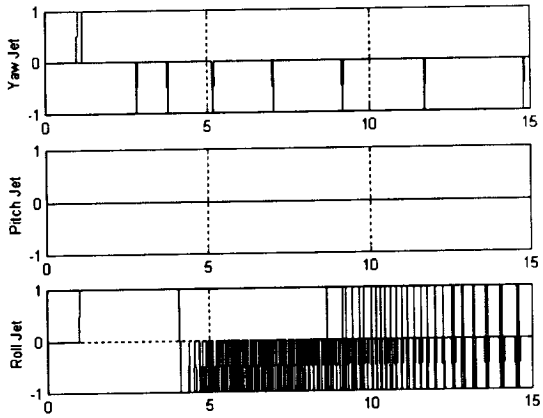

Figure 22 – Jet Firings in the upper trajectory for control

Jet firings are actually determined by a complex jet selection logic that determines which jets have failed and which are available for optimal control.

Robustness Analysis

The robustness of the X-37 design is assured in three ways. First, traditional gain and phase margin analysis is performed since there is a long history of successful aerospace programs using this methodology.

Second, using modern control tools, a mu analysis is performed after attaching the most important aerodynamic and mass properties uncertainties. The value of the mu analysis is that it simultaneously perturbs the uncertainties in the worst possible way to point out weaknesses in the design. Figure 23 shows just such a plot from the mu analysis. It can be seen that in this case there is no possible instability for the magnitude of the uncertainties attached, and the biggest contributors are the aerodynamic derivatives, $cn_{\delta a}$ and $cl_{\delta a}$.

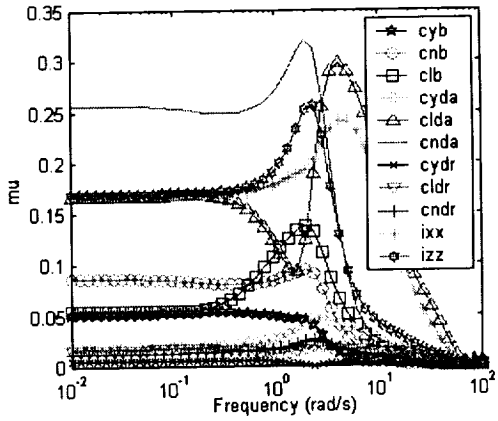

Figure 23 – Mu analysis showing relative contribution of each uncertainty

The third method to assure robustness, on the X-37, is to subject the whole design to a lot of stress cases on the 6DOF simulation. In these stress cases, numerous trajectory, aerodynamic, actuator, sensor, and mass property parameters are simultaneously varied. The performance of the vehicle along the trajectory is then assessed.

Conclusion

With the analysis and results presented in this paper, the X-37 has been shown to be a robust, aerospace vehicle. A trim analysis showed that there is excellent trim capability in all axes, and that after trimming there is enough surface authority left for control of the vehicle. The dynamics of the LCDP transition region were presented, and it was shown how the X-37 can be controlled in a region where aerodynamic alignments and uncertainties make the exact dynamics unknown. Results of the control design were presented and it was shown how the robustness of the design is ensured using classical and modern control methods.

References

[1]Nguyen, V., Chaudhary, A.K., Poladian, D.; " X-40A Guidance and Control and Flight Test Results," AAS paper no. 00-0015, February 3, 1999.

[2]Pamadi, B., "Performance, Stability, Dynamics, and Control of Airplanes," American Institute of Aeronautics and Astronautics, 1998.